Research Article

Forging optimisation process using numerical simulation and Taguchi method

Japeth Oirere Obiko[1] · **Fredrick Madaraka Mwema**[2] · **Harrison Shangwira**[2]

Received: 28 December 2019 / Accepted: 16 March 2020 / Published online: 19 March 2020

Abstract
This study reports on the optimisation of the forging process using Deform™ 3D simulation software and the Taguchi method. The forging simulation process was conducted on X20 steel used because of its application in boiler pipes in the fossil-fuel power plants. A three-level, three parameter Taguchi design of experiment for the Deform 3D simulations was used. The parameters considered for the simulations were cylinder (deformation) temperature, die speed and friction coefficient were studied. From the forging process, simulation results were analysed using Taguchi's orthogonal array. Further, ANOVA analysis was carried out to determine the significance of the parameters to the forging responses (maximum tensile stress and forging force). Results of the statistical analysis showed that the optimal parameters for improved product quality were deformation temperature of 1000 °C, die speed of v 20 mm/s and friction coefficient of 0.2. A confirmatory simulation was carried out using the optimal parameters. The simulation results verified that the optimal parameters showed a lower maximum tensile stress to 252.5 ± 2.5 MPa at the lateral surface of the deformed sample compared to other investigated conditions.

Keywords Forging process · Taguchi · Deform™ 3D · Forging load · Maximum tensile stress

1 Introduction

Over decades, metal forming processes such as forging extrusion and rolling have been used in the production of structural components [1–3]. Forged components find application in the automobile, aerospace and power plants [2, 4], which require high-quality products. During the forging process, material properties are altered due to large plastic deformation [5]. This is due to the higher application of axial forces leading to the multiaxial stress-state condition [6]. Hence, complex metal flow behaviour is experienced due to variation in the stress and strain distribution [7, 8]. Metal flow characteristics are sensitive to the forging parameters such as temperature, die speed, friction coefficient and the degree of deformation [9]. These forging parameters influence the final product quality [10]. In-depth understanding of metal flow pattern will enhance the production of a high-quality product. Therefore, optimisation of the forging parameters is of concern in improving the production process.

In the past, the manufacture of forged products was achieved through trial and error method and the experience of designers [11, 12]. This method was costly and time-consuming [12]. To improve product quality and increase productivity, computer and physical simulations have replaced the old technology [10, 13]. Physical simulation use laboratory specimens to study hot metal flow behaviour. The obtained flow stress data can be used for optimisation and prediction of the deformation process [14]. However, this method faces challenges due to the interfacial friction between the die and the workpiece. The interfacial friction leads to increased flow stress hence metal flow inhomogeneities [15–17]. Therefore, this method requires more experiments to determine the

✉ Fredrick Madaraka Mwema, fredrick.mwema@dkut.ac.ke | [1]Jomo Kenyatta University of Agriculture and Technology, Nairobi, Kenya. [2]Materials, Design & Manufacturing Group (MADEM), Department of Mechanical Engineering, Dedan Kimathi University of Technology, Nyeri, Kenya.

optimal conditions during the forging process. Hence, more experimental samples are required resulting in an expensive process. To cut-off production cost, commercial computer softwares have been developed to provide simulation tools for metal forming processes. Computer simulation software with Finite Element Method (FEM) tools provide a more reliable and less costly process for the optimisation of metalworking processes [18, 19]. For instance, Deform™ 3D simulation software has been widely used for the optimisation of the industrial forming processes [7, 20]. However, a series of simulations are required to achieve an optimised set of conditions for a given deformation process. The number of simulations can be reduced by applying the Design of Experiment (DoE) statistical techniques such as Taguchi's experimental design. This technique has been used to study the effects of process parameters and variables in the metal forming process [21, 22]. Taguchi design technique has been reported in the literature as an efficient tool for the optimisation of the production process [22]. To this end, literature has shown that Deform™ 3D software has been used for the simulation of the forging process of various metals and alloys [20, 23, 24]. Therefore, to reduce the simulation process, Taguchi's experimental method and Deform™ 3D simulation have been applied in this study to effectively study and optimise the forging process.

2 Simulation modelling

2.1 Forging material

Industrial forging process has been widely used for the production of structural components. However, the process is costly and time-consuming due to trial and error during the design stage. Recently, finite element methods have been utilised to simulation the forging process, hence optimise the forging process. In this study, forging simulation process was done using Deform™ 3D FEM software. Simulation data has been obtained using a 3D solid model of a short cylinder (ø8 mm and 12 mm long) of X20 creep resistant steel. The material properties are available in the Deform™ 3D database. Hence, the metal flow behaviour during the forging process was studied.

2.2 Design of experiment

Taguchi design approach provides an accurate and efficient way of understanding the interrelationships among parameters and their influence on the process. Therefore, this method enables optimisation of the production process by establishing a set of parameters that will improve the product quality. The key component during the design process lies in the selection of the control/independent factors. During the forging process, the main control factors are the workpiece (cylinder) temperature, the die speed and the coefficient of friction [17]. The control factors and the variable used in the simulation forging process are shown in Table 1. A three-level Orthogonal Array (OA) has been used leading to nine sets of simulations. The OA (L_9) employed in the simulation process is shown in Table 2. MINITAB 17 computer software has been used to design the simulation and analyse the simulation data.

Table 1 Simulation control factors and their different levels

Factor	Units	Symbol	Levels		
			1	2	3
Cylinder temperature	°C	T_c	800	900	1000
Die speed	mm/s	u_d	10	20	30
Friction coefficient	–	μ	0.1	0.2	0.3

Table 2 L9 orthogonal design array

Experiment No	Simulation control factors		
	T_c (°C)	u_d (mm/s)	μ
1	800	10	0.1
2	800	20	0.2
3	800	30	0.3
4	900	10	0.2
5	900	20	0.3
6	900	30	0.1
7	1000	10	0.3
8	1000	20	0.1
9	1000	30	0.2

2.3 Forging simulation model

The FEM Deform™ 3D software that is widely used in the simulation of hot working processes has been used in this study. The material properties of X20 steel were selected from the software database. The workpiece and die geometry were drawn using Deform™ 3D primitive geometry module. The mechanical properties of X20 steel are as follows: Young's modulus 200 GPa, Poissons' ratio 0.33, elongation 16% and density 7.7 g/mm^3. The meshed and deformed specimens are shown in Fig. 1. The simulation parameters/conditions are given in Table 3.

3 Results and discussion

3.1 Taguchi's experimental design

Metalworking processes such as forging described in this paper is influenced by the deformation loads and stresses. The interrelationship among the process parameters makes material flow pattern complex during forging

Fig. 1 Finite element model (**a**) meshed cylinder (**b**) deformed cylinder

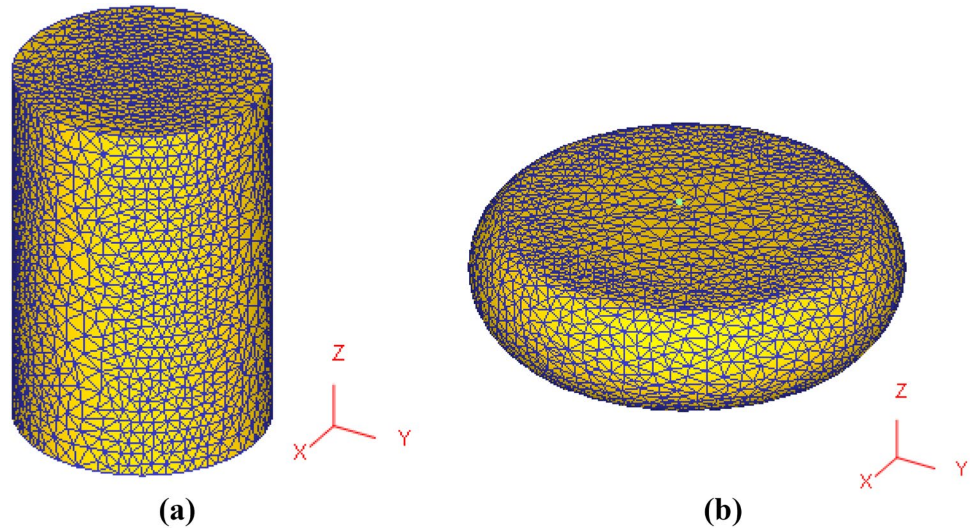

Table 3 Simulation conditions for the forging simulation process

No	Simulation parameter	Description
1	Specimen temperature (°C)	800–1000
2	Temperature of the Dies (°C)	100
3	Number of elements	33,164
4	Number of nodes	6924
5	Mesh type	Tetrahedral
6	Primary die	Top die
7	Simulation mode	Isothermal
8	Contact time (s)	1
9	Heat transfer coefficient (N/s/mm/°C)	5
10	Thermal conductivity (N/s/mm/°C)	0.02
11	Increment per step	
12	Environment temperature (°C)	20

and hence deformation analysis is not straightforward [6]. For instance, maximum tensile stresses occur at the lateral surface of the deformed sample during the forging process and these stresses result in sample cracking at the lateral surface during the deformation process [25]. Therefore, a high-quality product can be achieved through the optimisation of these two parameters. For the Taguchi design analysis, the forging load and the maximum tensile stress obtained from each forging simulation process was recorded for further analysis as shown in Table 4. Then, Taguchi response analysis of signal-to-noise (S/N ratio) quality characteristics of forging load and maximum tensile stress are also given in Table 4. According to Taguchi method, the highest S/N ratio represents a better quality. This implies that high-quality product can be achieved by the combination of the showing higher S/N ratio in Taguchi analysis. The S/N ratio of quality characteristic analysis for the two parameters (forging load and maximum tensile stress) with the objective of 'the smaller-the-better'. Very

Table 4 Simulation results for forging load (kN) and maximum tensile stress (MPa)

Exp. No	Cylinder temperature (°C)	Die speed (mm/s)	Friction coefficient (μ)	Forging force (kN)	Max tensile stress (MPa)	S/N ratios for applied force	S/N ratios for max tensile stress
1	800	10	0.1	60.298	461	−35.61	−53.27
2	800	20	0.2	55.906	261	−34.95	−48.33
3	800	30	0.3	59.728	502	−35.54	−54.01
4	900	10	0.2	47.193	397	−33.48	−51.98
5	900	20	0.3	46.003	354	−33.26	−50.98
6	900	30	0.1	45.778	329	−33.21	−50.34
7	1000	10	0.3	38.850	282	−31.79	−49.01
8	1000	20	0.1	34.967	270	−30.87	−48.63
9	1000	30	0.2	34.638	277	−30.79	−48.85

Table 5 S/N response table for maximum stress and force

Levels	Control factors					
	Maximum tensile stress (MPa)			Maximum force (kN)		
	Temperature	Speed	Friction coefficient	Temperature	Speed	Friction coefficient
1	−51.87	−51.42	−50.75	−35.36	−33.62	−33.23
2	−51.10	**−49.31**	**−49.72**	−33.32	**−33.03**	**−33.07**
3	**−48.83**	−51.07	−51.33	**−31.15**	−33.18	−33.52
Delta	3.05	2.10	1.61	4.21	0.60	0.45
Rank	1	2	3	1	2	3

The bold values are the largest values of the S/N ratios

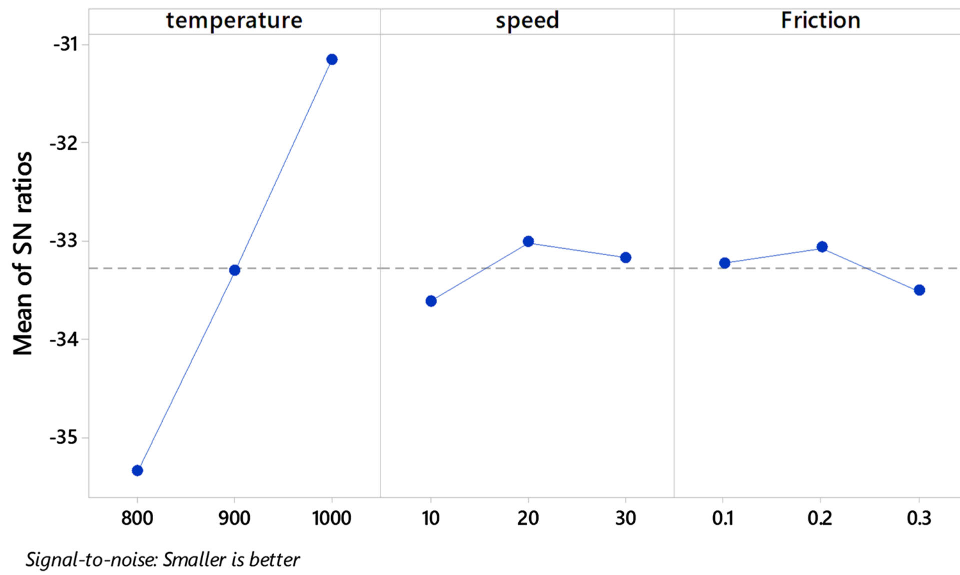

Fig. 2 Main effects plots for S/N ratios of the applied force during forging simulation

high stresses lead to extreme deformations and hence high strain variation and defects. Table 5 shows the S/N responses for maximum stress and force and the results here indicate the optimal levels of the control factors for both the dependent parameters. These results are further shown in graphical form in Figs. 2 and 3. From these graphs, the optimal control parameters for minimizing the stresses and loads during a forging process can easily

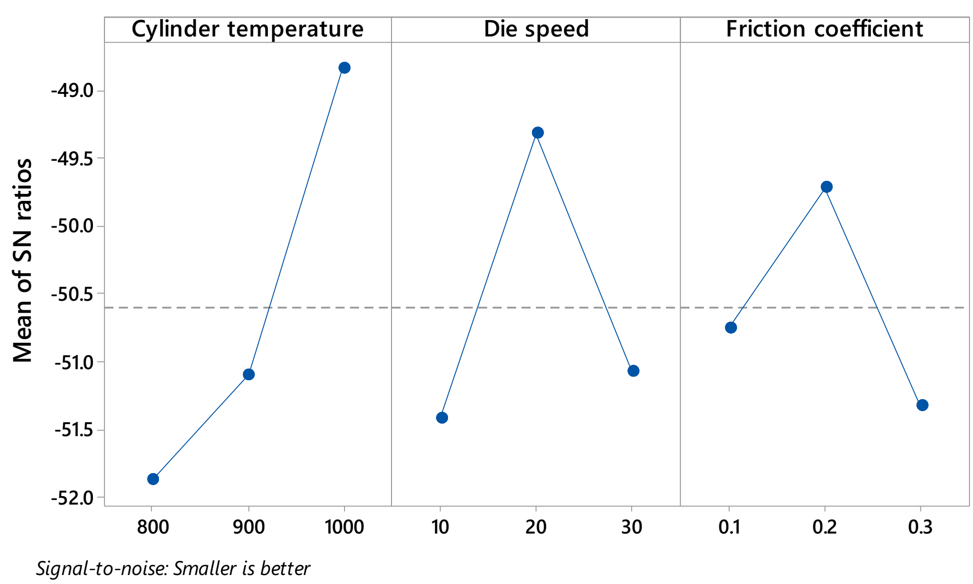

Fig. 3 Main effects plots for S/N ratios of the maximum tensile stress during forging simulation

Table 6 Results of ANOVA for maximum forging forces and tensile stresses

Factor	Degree of freedom	Sum of squares	Mean squares	% contribution	F-value	*P*-Value
Maximum force						
Cylinder temperature	2	761.16	380.58	97.00	2363.9	0.00
Die speed	2	15.41	7.70	1.96	47.85	0.02
Friction coefficient	2	7.81	3.91	1.00	24.25	0.04
Error	2	0.322	0.161	0.04		
Total	8	784.7		100		
Maximum tensile stress						
Cylinder temperature	2	26,640	13,320	42.7	1.68	0.373
Die speed	2	12,864	6432	20.6	0.81	0.552
Friction coefficient	2	6991	3495	11.2	0.44	0.694
Error	2	15,838	7919	25.4		
Total	8	62,333		100		

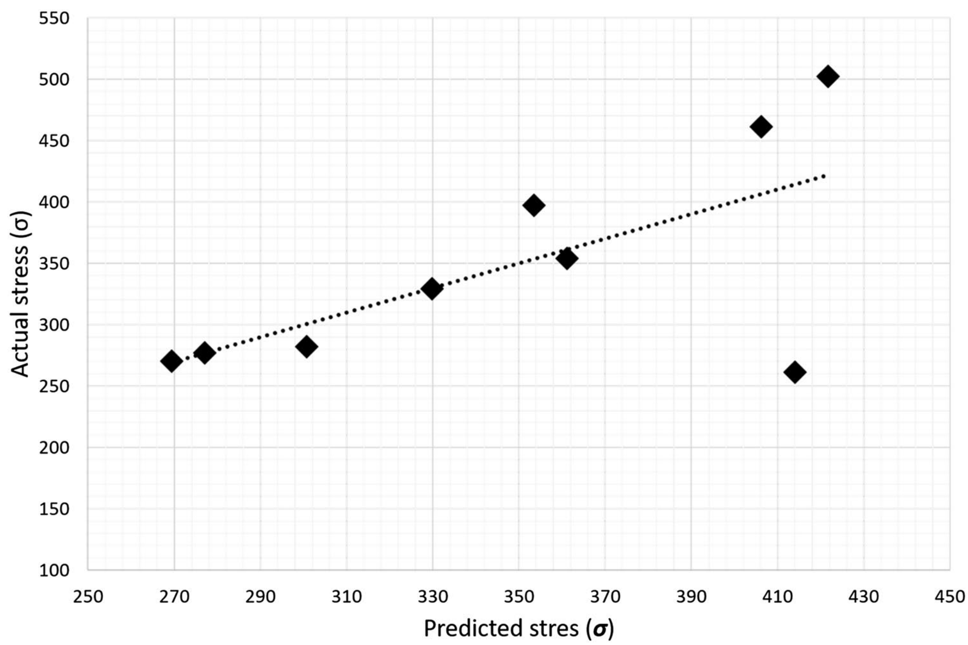

Fig. 4 Comparison of the actual maximum stresses from the simulation to the linear regression model

be obtained from Table 5 and Figs. 2 and 3. The optimum level for the forging process was obtained at the cylinder temperature of 1000 °C, upper die speed of 20 mm/s and friction coefficient of 0.2 according to these results. The selected levels had the highest S/N ratio compared to the other levels.

3.2 ANOVA

The influence of forging parameters was further analysed using Analysis of Variance (ANOVA) as shown in Table 6. This technique provides a means of testing the statistical hypothesis of complex occurrences with multivariate data. As seen in the table, the *P*-value shows the differences in the forging factors. The obtained results indicate that the differences in the factors were highly significant for the maximum forging load. The cylinder temperature had the highest per cent contribution (97%) with the lowest *P*-value of less than 0.001 compared to the other factors. This implies that the cylinder temperature plays a key role during deformation. The final quality of the product will be affected by the deformation temperature. The microstructure formation and refinement (due to dynamic softening) mainly depends on the forging parameters such as the deformation temperature and strain rate (strain rate is given by dividing the die speed by the deformed sample height). The coefficient of friction had the lowest per cent contribution (1.00%) to the forging load. However, the friction coefficient affects (increases the forging loads) the forging loads leading to inhomogeneous metal flow

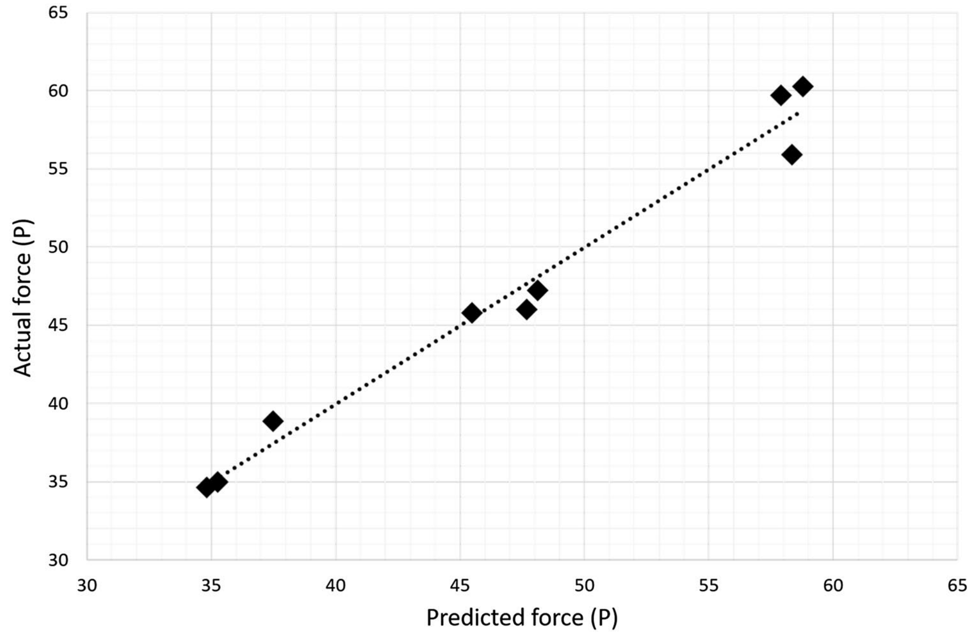

Fig. 5 Comparison of the actual maximum force from the simulation to the linear regression model

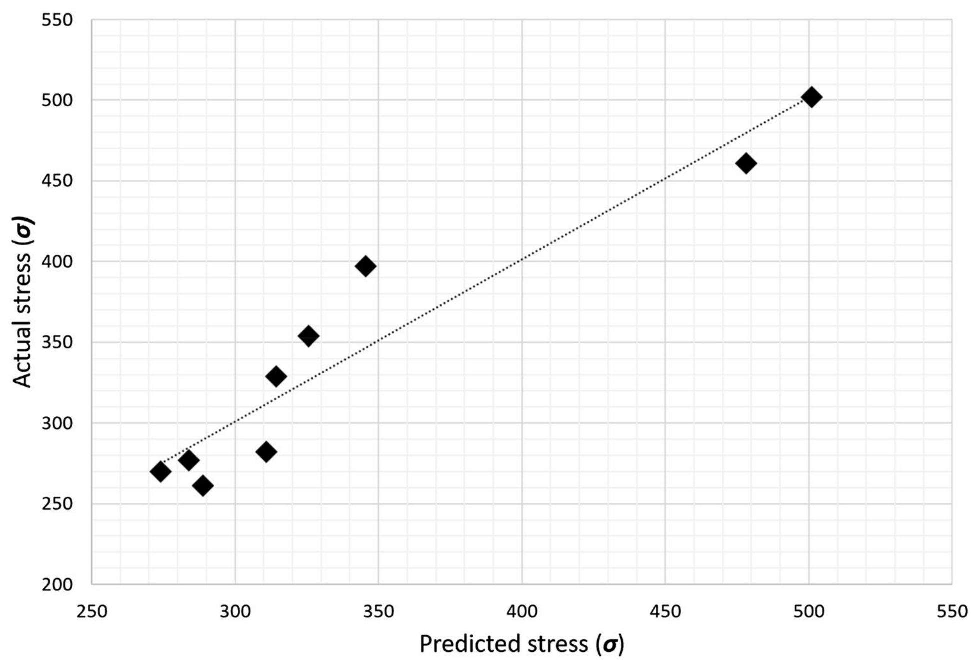

Fig. 6 Comparison of the actual maximum stresses from the simulation to the quadratic regression model

behaviour [15]. The analysis has shown that the three factors affect the forging load hence the deformation process. For the case of maximum tensile stress, the considered control forging factors exhibit little contribution. It can further be seen that all the *P*-values were greater than 0.05, indicating an insignificant relationship. The general observation is that there is no dominating factor of the three considered here in controlling the forging stress. Therefore, the authors cannot conclude that a significant difference exists.

3.3 Regression analysis of maximum forging force and tensile stress

To investigate relationship between dependent and independent variables, regression analyses were utilized in this work. As mentioned, the dependent factors in this

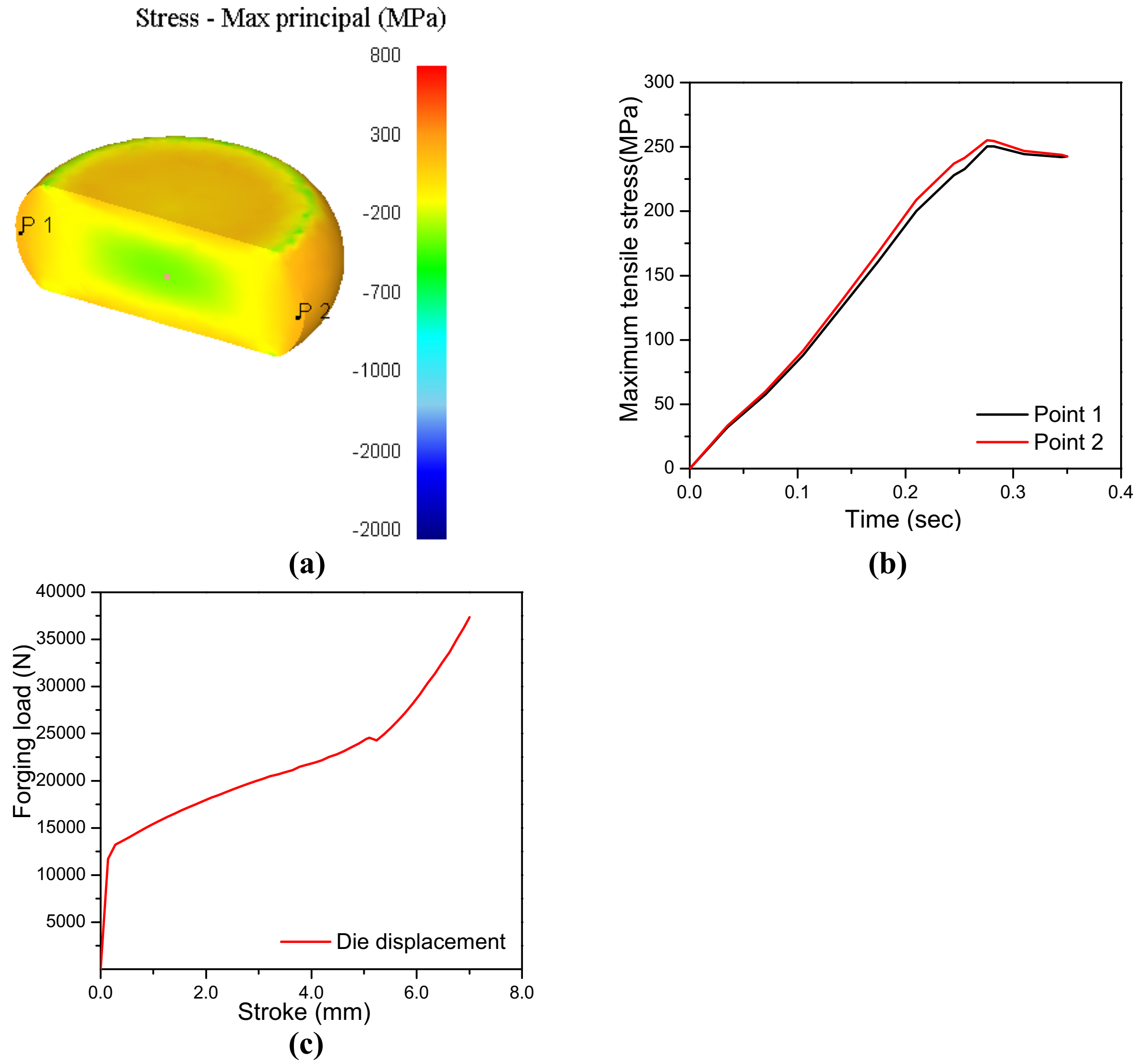

Fig. 7 **a** Deformed sample using optimised conditions, plots of (**b**) maximum tensile stress at point 1 and 2 against time and (**c**) forging loads against stroke during the forging process

work are maximum force (**P**) and maximum tensile stress (**σ**) whereas, the independent variables are cylinder temperature (**T**), forging speed (**S**) and coefficient of friction at the tool-sample interface (**μ**). The predictive equations from the linear regression analysis for maximum stress and forging forces are as follows represented below.

$$\sigma = 925 - 0.658T - 0.53S + 130\mu \tag{1}$$

$$P = 149.14 - 0.11246T - 0.1033S + 5.90\mu \tag{2}$$

Plots comparing the predicted and the actual simulation results of stresses and load are shown in Figs. 4 and 5 for the linear regression analyses. As shown, from the regressions, the R^2 values obtained are 0.44 and 0.98 for maximum tensile stress and maximum force respectively. The linear model (Eq. 2) can therefore satisfactorily predict the forces in the Deform 3D simulation of a forging process. On contrary, the R^2 value for maximum stress is very low and thus the prediction model shown in Eq. 1 cannot be relied upon to predict the maximum stresses during a forging process. As such, quadratic regression modelling was applied for maximum tensile stress prediction and the optimal model is represented in Eq. 3.

$$\begin{aligned}\sigma = {} & 805 + 0.000413T^2 + 0.871S^2 + 6675\mu^2 \\ & - 0.0551TS - 4.39T\mu - 129S\mu + 0.220TS\mu\end{aligned} \tag{3}$$

The regression model in Eq. 3 and plot in Fig. 6 reveal that quadratic regression model is more reliable to predict the maximum tensile stress during a forging process ($R^2 = 0.91$).

3.4 Forging simulation after optimisation

Figure 7 shows the forging simulation results obtained after using the optimal forging parameters obtained from Figs. 2, 3 and Table 5. The optimal parameters were applied in Deform™ 3D simulation process to confirm the Taguchi experimental design and optimisation procedure. The results show the values of the forging load and the maximum tensile stress. The forging load was 37.42 kN and the maximum tensile stress at points 1 and 2 on the lateral surface of the deformed sample in Fig. 7a were ranging between 255 and 250 MPa. The maximum tensile stress obtained was much lower than those shown in Table 4. This value shows that the principal stress at the lateral side of the sample is lower than the ultimate tensile stress (430 MPa) of X20 power plant steel after 130000 h for service temperature of 530 °C [26–29].

4 Conclusion

The optimisation of the forging process was conducted using Taguchi design of finite element Deform™ 3D simulation results. The three forging factors used for the analysis were the cylinder temperature, die speed and the coefficient of friction. A series of finite element method simulations were conducted based on Taguchi experimental design and optimisations were later conducted through ANOVA and regression analyses. The results showed that the forging parameters have a significant difference with the responses (forging load and the maximum tensile stress). The cylinder (deformation) temperatures had the highest contribution of 97% to the forging load hence, affecting the forging process. However, the forging factors did not show significant differences to the maximum tensile stress. Both linear and quadratic regression models were used to predict the dependent factors and it was shown that maximum force can be predicted using the linear regression whereas the maximum stress can be accurately predicted using high-order regression models. Simulation analysis was further done to verify the obtained optimal parameters during the forging process. The simulation results verified that the optimal parameters lower the maximum tensile stress of the deformed sample.

Compliance with ethical standards

Conflict of interest The authors declare no conflict of interest.

References

1. Osakada K (2007) Effects of strain rate and temperature in forming processes of metals. Le J Phys IV 07(C3):C3-XXXVII-C3-XLIV
2. Lu SQ, Li X, Wang KL, Liu SB, Fu MW (2013) A method for prediction of unstable deformation in hot forging process by simulation. Trans Nonferrous Met Soc China 23(12):3739–3747
3. Evans RW, Scharning PJ (2001) Axisymmetric compression test and hot working properties of alloys. Mater Sci Technol 17(8):995–1004
4. Lee YS, Lee SU, Van Tyne CJ, Joo BD, Moon YH (2011) Internal void closure during the forging of large cast ingots using a simulation approach. J Mater Process Technol 211:1136–1145
5. Rasti J, Najafizadeh A, Meratian M (2011) Correcting the stress-strain curve in hot compression test using finite element analysis and Taguchi method. Int J ISSI 8(1):26–33
6. George D (1988) Mechanical metallurgy. Mcgraw-Hill Book Company, New York
7. Lin YC, Chen MS, Zhong J (2008) Numerical simulation for stress/strain distribution and microstructural evolution in 42CrMo steel during hot upsetting process. Comput Mater Sci 43(4):1117–1122
8. Obiko JO, Mwema FM, Akinlabi ET (2019) Strain rate-strain/stress relationship during isothermal forging: a deform-3D FEM. Eng Solid Mech 8:1–6
9. Kingkam W, Li N, Zhang HX, Zhao CZ (2017) Hot deformation behavior of high strength low alloy steel by thermo mechanical simulator and finite element method. IOP Conf Ser Mater Sci Eng 205(1):012001
10. Ajeet Babu PK, Saraf MR, Vora KC, Chaurasiya MS, Kuppan P (2015) Influence of forging parameters on the mechanical behavior and hot forgeability of aluminium alloy. Mater Today Proc 2(4–5):3238–3244
11. Moraes ALI, Balancin O (2015) Numerical simulation of hot closed die forging of a low carbon steel coupled with microstructure evolution. Mater Res 18(1):92–97
12. Maarefdoust M (2012) Simulation of finite volume of hot forging process of industrial gear. Int Proc Comput Sci Inf Technol 57(Icni):111–115
13. Na YS, Yeom JT, Park NK, Lee JY (2003) Simulation of microstructures for Alloy 718 blade forging using 3D FEM simulator. J Mater Process Technol 141(3):337–342
14. Shi L, Yang H, Guo LG, Zhang J (6005A) Constitutive modeling of deformation in high temperature of a forging 6005A aluminum alloy. Mater Des 54:576–581
15. Li YP, Onodera E, Matsumoto H, Chiba A (2009) Correcting the stress-strain curve in hot compression process to high strain level. Metall Mater Trans A Phys Metall Mater Sci 40(4):982–990
16. Obiko JO, Mwema FM, Bodunrin MO (2019) Finite element simulation of X20CrMoV121 steel billet forging process using the deform 3D software. SN Appl Sci 1(9):1044
17. Lin SY (1995) An investigation of die-workpiece interface friction during the upsetting process. J Mater Process Tech 54(1–4):239–248
18. Ketabchi M, Mohammadi H, Izadi M (2012) Finite-element simulation and experimental investigation of isothermal backward extrusion of 7075 Al alloy. Arab J Sci Eng 37(8):2287–2296
19. Mohapatra SK, Maity KP (2016) Parametric optimization of simulated extrusion of square to square section through linear converging die. IOP Conf Ser Mater Sci Eng 115(1):012031
20. Zhang ZJ, Dai GZ, Wu SN, Dong LX, Liu LL (2009) Simulation of 42CrMo steel billet upsetting and its defects analyses during forming process based on the software DEFORM-3D. Mater Sci Eng A 499(1–2):49–52

21. Ohdar R, Equbal MI, Kumar V (2013) Die stress optimization using finite element and Taguchi method. Mater Sci Forum 762:319–324
22. Deepak Kumar S, Karthik D, Mandal A, Pavan Kumar JSR (2017) Optimization of Thixoforging process parameters of A356 alloy using Taguchi's experimental design and DEFORM Simulation. Mater Today Proc 4(9):9987–9991
23. Ren J, Wang W, Liu R (2011) Optimization design based on DEFORM-3D finite element analysis about steel rolling production. Key Eng Mater 480–481:1079–1084
24. Su YL, Yang WZ, Wang CP (2013) Upsetting process analysis and numerical simulation of metal pipe's end. Appl Mech Mater 364:488–492
25. Yang ZN, Dai LQ, Chu CH, Zhang FC, Wang LW, Xiao AP (2017) Effect of aluminum alloying on the hot deformation behavior of nano-bainite bearing steel. J Mater Eng Perform 26(12):5954–5962
26. Straub S, Blum W, Rattger D, Polcik P, Eifler D, Borbely A, Ungar T (1997) Microstructural stability of the martensitic steel X20CrMoV12·1 after 130000 h of service at 530. Mater Technol 68(8):368–373
27. Mwema FM, Obiko JO, Akinlabi ET, Akinlabi SA, Fatoba OS (2019) Effect of punch force on the upsetting deformation process using three-dimensional finite element analysis. J Phys Conf Ser 1378(3):032094
28. Liu XG, Ji HP, Guo H, Jin M, Guo BF, Gao L (2013) Study on hot deformation behaviour of 316LN austenitic stainless steel based on hot processing map. Mater Sci Technol 29:24–29
29. Han Y, Sun Y, Zhang W, Chen H (2017) Hot deformation and processing window optimization of a 70MnSiCrMo carbide-free bainitic steel. Materials (Basel) 10(3):318